AGU PUBLICATIONS

Geophysical Research Letters

RESEARCH LETTER
10.1002/2015GL064841

Key Points:
- Development of a method to calculate the curl of the ionospheric magnetic field
- Use on nighttime data from Swarm satellites flowing at different altitudes
- Estimation of the vector components of the density current in the *F* region

Correspondence to:
R. Tozzi,
roberta.tozzi@ingv.it

Citation:
Tozzi, R., M. Pezzopane, P. De Michelis, and M. Piersanti (2015), Applying a curl-B technique to Swarm vector data to estimate nighttime *F* region current intensities, *Geophys. Res. Lett.*, *42*, 6162–6169, doi:10.1002/2015GL064841.

Received 8 JUN 2015
Accepted 2 JUL 2015
Accepted article online 4 JUL 2015
Published online 10 AUG 2015

Applying a curl-B technique to Swarm vector data to estimate nighttime *F* region current intensities

Roberta Tozzi[1], Michael Pezzopane[1], Paola De Michelis[1], and Mirko Piersanti[2]

[1]Istituto Nazionale di Geofisica e Vulcanologia, Rome, Italy, [2]Dipartimento di Scienze Chimiche e Fisiche, Università degli Studi dell'Aquila, L'Aquila, Italy

Abstract The innovative geometry of European Space Agency Swarm constellation opens the way for new investigations based on magnetic data. Since the knowledge of a vector field on two spherical surfaces allows calculating its curl, we propose a new technique to estimate the curl of the ionospheric magnetic field measured by Swarm satellites A and B, orbiting the Earth at two different altitudes from March to September 2014. Using this technique, we mapped the amplitude of the radial, meridional, and zonal components and of total intensity of the ionospheric current density at the satellite's altitudes, i.e., the *F* region of the ionosphere, during two local nighttime intervals: before and after midnight. Most of the obtained results are consistent with some of the known features of nighttime *F* region currents; others need further investigation. The proposed technique could contribute in selecting magnetic data with minimum contamination from nighttime *F* region electric currents for magnetic modeling purposes.

1. Introduction

In the last decade, the understanding of the geomagnetic field has experienced a strong impulse due to the large amount of continuous observations provided from satellite missions, particularly the Ørsted mission by the Danish Meteorological Institute and the CHAMP mission by the GeoForschungsZentrum at Potsdam (details are available at http://www.space.dtu.dk/english/Research/Projects/Oersted and http://op.gfz-potsdam.de/champ/index_CHAMP.html, respectively). At the end of 2013 a new era in magnetic observations from satellites began with the successful launch by European Space Agency (ESA) of the three-satellite Swarm constellation. The innovation introduced by this mission lays certainly in the high-resolution magnetometers and in the other instruments installed on board the three satellites and above all in its geometrical configuration. In fact, two satellites are orbiting the Earth in tandem at the same altitude (Alpha and Charlie) while the third (Bravo) is flying at a higher altitude, about 50 km above Swarm A and C and, in the course of its life, its orbital plane will gradually get farther from those of the other two satellites.

Besides the new possibilities of investigation related to high-resolution observations, measurements of the geomagnetic field on two spherical surfaces (Swarm A/C and B) and along two nearby orbits (Swarm A and C) can allow the development of new methods of analysis of the Earth's magnetic field. In particular, differential operators, as the curl of the magnetic field Swarm satellites go through, can be estimated directly from measured data. One of the first reconstructions of ionospheric *F* region currents was made by *Olsen* [1997] using data from Magsat and decomposing the magnetic field into toroidal and poloidal parts to achieve the radial current component and, under a series of assumptions, also the horizontal current density. A technique to recover the vertical component of field-aligned current density through a curl-B technique applied to the upcoming Swarm observations has been proposed by *Ritter and Lühr* [2006] who simulated Swarm magnetic data. The same method has been recently applied on real Swarm magnetic data to estimate *F* region currents at low latitudes [*Lühr et al.*, 2015]. Differently, *Shore et al.* [2013] have combined data from Ørsted and CHAMP satellites for the years 2001–2006 and applied Ampere's law to estimate the zonal current flowing in the spherical shell delimited by satellite's orbits. The importance of these techniques relates to the possibility to quantify electric currents in which satellites are immersed while measuring the geomagnetic field. If, on one side, the observation of the Earth's magnetic field by low Earth orbit satellites offers a spatial coverage that ground magnetic observations will never be able to provide, on the other side they measure magnetic field in regions where electric currents flow and are therefore not free from magnetic field sources. This implies that magnetic field can no longer be expressed in terms of the gradient of a scalar potential and all representations based on this assumption lose their validity. One of the methods to minimize the consequences of this issue

is to consider nighttime data, i.e., when currents are supposed to be small. In this letter, we propose a new method for the complete estimation of the curl of the ionospheric magnetic field, and therefore of current density, and show its application right to nighttime Swarm magnetic vector data.

After selecting Swarm magnetic data measured under low-level geomagnetic activity conditions, nighttime geomagnetic field of ionospheric origin is obtained using magnetic global models. Results, consisting of densities of electric currents flowing at the Swarm altitudes, i.e., of the *F* region of the ionosphere, are discussed. Even though data selection is made using geomagnetic indices (*Kp* and *Dst*) that are optimal for low and middle latitudes, we find interesting results also for current systems typical of the high latitudes as, for instance, the field-aligned currents. Anyway, an in-depth study of these currents would require different geomagnetic indices for data selection (e.g., *AE*) as well as to cope with the dependence on interplanetary magnetic field and season [*Green et al.*, 2009], all issues that are beyond the scope of this letter but that will be investigated in a separate work.

In the following section 2 the method is explained and results coming from its application to Swarm vector magnetic data are discussed, while in section 3 main points and future developments are summarized.

2. Data Processing

Data used for this study are vector magnetic measurements recorded by two of the three satellites of Swarm constellation. Time interval analyzed ranges from 15 March to 28 September 2014. During this period Swarm A has flown along an almost polar orbit at a stable altitude of ~470 km that was reached at the end of February, while Swarm B has flown at a stable altitude of ~520 km reached at mid-March. We use low-resolution (i.e., 1 Hz sampling) level 1b magnetic data collected on Swarm A and B that according to ESA nomenclature are named SW_OPER_MAGx_LR_1B ($x = A, B$) with file counter equal to 0302 when available and 0301 otherwise, in the NEC (North-East-Center) frame.

As already mentioned we describe and apply a new method to calculate the curl of a vector field to geomagnetic field of ionospheric origin, thus estimating the intensity of the current flowing in the spherical shell delimited by Swarm constellation. To separate the ionospheric component of geomagnetic field from those generated by irregular magnetospheric sources, we keep only measurements made under conditions characterized by values of $Kp \leq 2^0$ and of $|Dst| \leq 15$ nT [*Chambodut et al.*, 2002]. We choose these two geomagnetic indices to discriminate between different levels of magnetospheric activity at low and middle latitudes because they reflect the level of worldwide geomagnetic activity (*Kp*) and the effect on the ground due to the ring current intensity (*Dst*). The selected values of geomagnetic indices permit us to include in our analysis only geomagnetically quiet periods, when the strength of the external irregular magnetic fields is low. It is worth, here, mentioning that the choice of data on the base of magnetic indices does not completely guarantee from not including in the analysis ionospheric perturbations that have a signature on magnetic data as, for instance, spread *F*. This phenomenon has been shown to have a very high occurrence rate (up to 80%) during the winter period and a much lower occurrence rate (13.2%) during the other seasons [*Stolle et al.*, 2006]. Taking into account the time coverage of data here considered, i.e., spring and summer periods, possible effects of spread *F* on magnetic residuals will not be taken into account.

Once a set of measurements corresponding to quiet geomagnetic conditions has been obtained, in order to investigate ionospheric magnetic field, fields generated by other sources as core, crust, and magnetosphere have to be removed.

The first consists of removing the main field by means of CHAOS-5 model, the crustal field by means of MF7, and the magnetospheric field by means of Tsyganenko model T01 [*Tsyganenko*, 2002a, 2002b]. CHAOS-5 [*Finlay et al.*, 2015] is the newest version of the CHAOS series of geomagnetic field models [*Olsen et al.*, 2014] and describes the main field; it is used for degrees 1 to 20; code and documentation with details on the model are available at http://www.spacecenter.dk/files/magnetic-models/CHAOS-5/.

MF7 is an updated version of a previous model [*Maus et al.*, 2008] and is capable of resolving crustal magnetic field from spherical harmonic degrees 16 to 133; only degrees greater than 20 are considered to avoid the overlapping with CHAOS-5. Model and related information can be found at http://www.geomag.us/models/MF7.html.

To remove from our data the contribution of regular magnetospheric currents, which cannot be entirely avoided by selecting quiet periods [*Lui*, 2001], we use Tsyganenko model T01. It is a semiempirical best fit

representation for the magnetic field, based on a large number of satellite observations (e.g., IMP, HEOS, ISEE, Polar, Geotail, and GOES) and includes the contributions from major external magnetospheric sources: ring current, magnetotail current system, magnetopause currents, and large-scale system of field-aligned currents. Although T01 is an empirical model, the use of 1 min values of input parameters such as the solar wind (SW) dynamic pressure, the azimuthal and northward components of the interplanetary magnetic field (IMF), and *Dst* index accounts for the varying SW and IMF conditions for the prediction of the magnetospheric field [*Villante and Piersanti*, 2008].

The second approach consists of using CHAOS-5 for removal of main, crustal, and magnetospheric fields. Indeed, CHAOS-5 models not only magnetic field of internal origin up to spherical harmonic degree 90, thus including crustal field, but also part of the magnetospheric field. In detail, the external field modeled by CHAOS-5 includes contributions by the ring current (up to spherical harmonic degree $n = 2$) and by magnetotail and magnetopause currents (up to spherical harmonic degree $n = 2$ and order $m = 0$). The index used to estimate the strength of ring current is the *RC* index [*Olsen et al.*, 2014]. So far, CHAOS-5 models the magnetospheric field only up to 28 September 2014; this explains the upper bound of the time interval investigated in this work. Comparing the ionospheric field obtained in the two cases, we observe that Tsyganenko model (first approach) tends to overestimate the contribution of ring current thus producing markedly positive residuals of the northward component over all equatorial and midlatitude band. This hides the small magnetic field of ionospheric origin. On the contrary, removal of undesired contributions based exclusively on CHAOS-5 (second approach) produces robust residuals on which the analysis that follows is based on. The differences in the results are possibly related to the different conceiving of these two models: Tsyganenko is almost an empirical model based primarily on equations governing processes in the whole magnetosphere and is preferable when looking for an overall average picture of magnetospheric field. On the other hand, CHAOS-5 is a data assimilation model that utilizes magnetic data measured by satellites and by ground observatories. This makes it able to better represent the low-degree magnetospheric field due mainly to the ring current.

It is also custom to keep data only from dark regions, with the Sun zenith angle less than 101.54° [*Thomson and Lesur*, 2007]. However, considering the time period of observation (from March to September), this further selection would lead to a partial coverage of the Southern Hemisphere; therefore, it is not applied.

Data are converted from NEC frame to spherical frame (θ being colatitude, ϕ longitude, and r radial distance from the center of the Earth) and grouped into two subsets consisting of B_θ, B_ϕ, and B_r (i.e., meridional, azimuthal, and radial, respectively) components of the ionospheric magnetic field according to the value of two local time (LT) intervals: 19–23 LT and 01–05 LT. In this way, time variations occurring during the night can be recognized. Measurements of each subset are grouped, according to their coordinates (θ and ϕ) in 5° × 5° bins to cover the entire range of colatitudes and longitudes (36 bins in latitude and 72 in longitude). Values of B_θ, B_ϕ, and B_r falling in each bin for both Swarm A and B are averaged, and matrices with elements $B_{\theta x}^{j,k}$, $B_{\phi x}^{j,k}$, and $B_{rx}^{j,k}$ with $j = 1, \ldots, 36$, $k = 1, \ldots, 72$, and $x = A$ or B are created. Values of the radial distance from the Earth are stored, following the same procedure, into two matrices with elements $R_A^{j,k}$ and $R_B^{j,k}$. On all the matrices it is applied a low-pass Gaussian filter with a cutoff frequency corresponding to scale lengths of about 3500 km. The choice to focus on large scales depends on the present spatial coverage of Swarm data in combination with the need to look inside restricted LT windows that reduces the number of total observations. A smaller bin size implies the presence of empty bins in matrices and, in general, a smaller number of measurements within each bin with the consequence of less robust statistics. Figure 1 shows the number of measurements falling in each bin for each satellite and LT interval. To have an idea of the robustness of the matrices, we estimated the relative error associated to each matrix element as dm/m, where m is the average value associated to each bin (i.e., $m = B_{\theta x}^{j,k}, B_{\phi x}^{j,k}, B_{rx}^{j,k}$) and $dm = \sigma/\sqrt{n}$ is the error associated to the average m (being σ the standard deviation of the n measurements within each bin). The relative errors have been estimated for measurements from both Swarm A and B, both LT intervals, and all magnetic components. On average, the relative error associated to the mean results to be less than 18% for 80% of measurements and less than 35% for 90% of measurements. Although these values are not small, they support the robustness of the average values used to build the matrices described above.

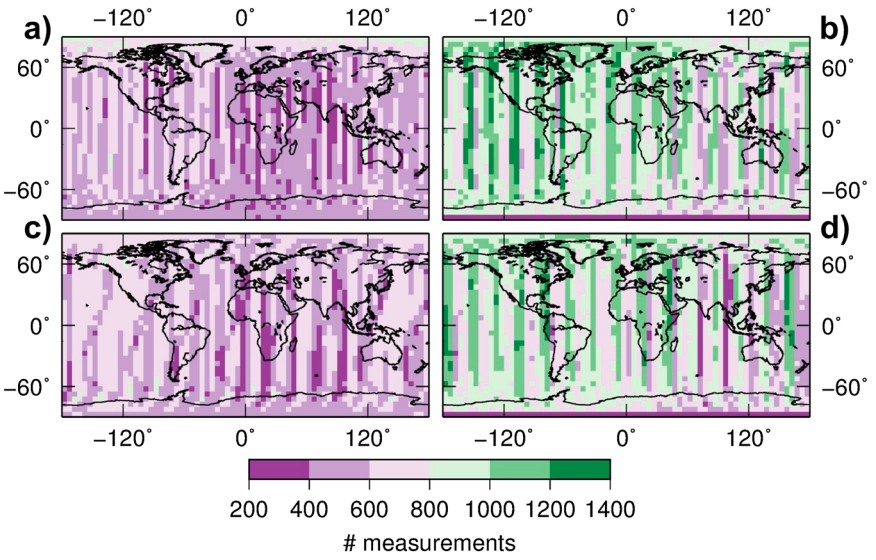

Figure 1. Number of measurements used to estimate the matricial elements $B^{j,k}_{\theta x}$, $B^{j,k}_{\phi x}$, and $B^{j,k}_{rx}$ ($j = 1, ..., 36$, $k = 1, ..., 72$, and $x = A$ or B) for Swarm A and B in the (a and c) 19–23 LT and (b and d) 01–05 LT time intervals, after selection for *Kp* and *Dst* indices.

3. Analysis and Results

As described in the previous section we reconstruct the ionospheric magnetic field observed on the surface of a spherical shell during two LT intervals. For the reasons explained in section 2 the analysis that follows is made on magnetic field residuals obtained using the approach based exclusively on CHAOS-5 model.

Under general conditions the current density can be derived from the fourth Maxwell equation. Since in the ionosphere the vacuum displacement current $\epsilon_0 \partial \mathbf{E}/\partial t$ is small with respect to conduction current **J**, it can be neglected [*Kelley*, 2009]. Under these assumptions, current density **J** flowing inside the shell covered by Swarm A and B can be expressed by

$$\mathbf{J} = \frac{1}{\mu_0} \nabla \times \mathbf{B} \tag{1}$$

where μ_0 is vacuum magnetic permeability and **B** magnetic field. In practice, to estimate the components of the current density in the spherical frame, i.e., J_θ, J_ϕ, and J_r, we introduce the following formulas to translate the curl operator in terms of discrete observed data (in this case values of the magnetic field of ionospheric origin at the two altitudes of Swarm A and B satellites):

$$j^{j,k}_r = \frac{1}{\mu_0} \frac{1}{R^{j,k}_A \sin\theta_j} \left[\frac{\sin\theta_{j+1} B^{j+1,k}_{\phi A} - \sin\theta_j B^{j,k}_{\phi A}}{\Delta\theta} - \frac{B^{j,k+1}_{\theta A} - B^{j,k}_{\theta A}}{\Delta\phi} \right] \tag{2}$$

$$j^{j,k}_\theta = \frac{1}{\mu_0} \frac{1}{R^{j,k}_A} \left[\frac{B^{j,k+1}_{rA} - B^{j,k}_{rA}}{\sin\theta_j \Delta\phi} - \frac{R^{j,k}_B B^{j,k}_{\phi B} - R^{j,k}_A B^{j,k}_{\phi A}}{R^{j,k}_B - R^{j,k}_A} \right] \tag{3}$$

$$j^{j,k}_\phi = \frac{1}{\mu_0} \frac{1}{R^{j,k}_A} \left[\frac{R^{j,k}_B B^{j,k}_{\theta B} - R^{j,k}_A B^{j,k}_{\theta A}}{R^{j,k}_B - R^{j,k}_A} - \frac{B^{j+1,k}_{rA} - B^{j,k}_{rA}}{\Delta\theta} \right] \tag{4}$$

where $\Delta\theta$ and $\Delta\phi$ are the bin widths in colatitude and longitude; that is, $\Delta\theta = \Delta\phi = 5°$ (to evaluate equations (2)–(4), degrees are converted into radians). From the three components of current density it is then straightforward to estimate its total intensity for both the 19–23 LT and 01–05 LT time intervals.

To evaluate the validity of this method, we draw maps of the large-scale current density obtained using equations (2)–(4) directly with Swarm data and examine the features of the radial (J_r), meridional (J_θ), and zonal (J_ϕ) components and of its total intensity $|J|$. These maps are shown in Figure 2.

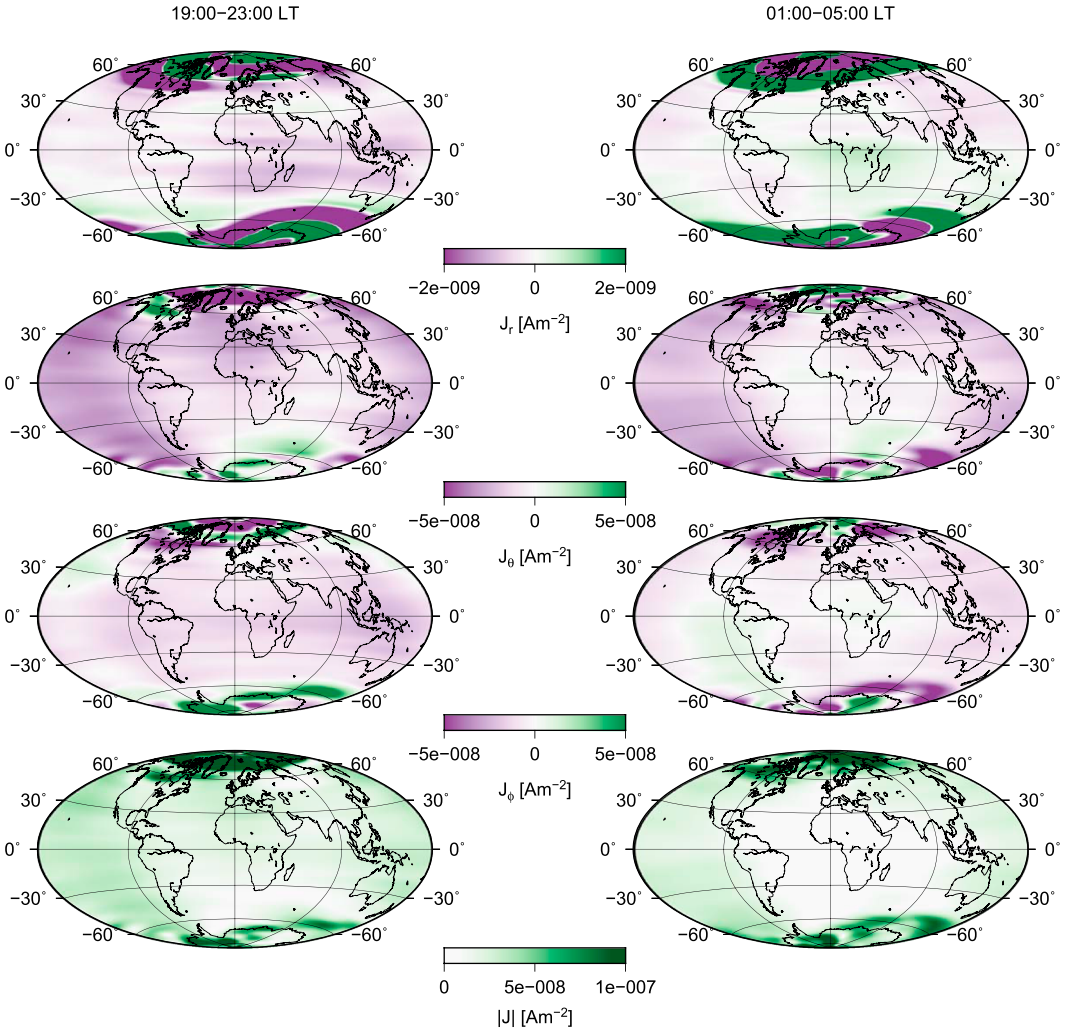

Figure 2. Large-scale current density obtained by estimating the curl of the residual magnetic field of ionospheric origin between the altitudes of Swarm A and B satellites. (first row) Radial component J_r (positive outward), (second row) meridional component J_θ (positive southward), (third row) zonal component J_ϕ (positive eastward), and (fourth row) total intensity $|J|$; (left column) maps referring to 19–23 LT and (right column) maps referring to 01–05 LT. Period of observation: from 15 March to 28 September 2014.

Focusing on low and middle latitudes, we observe a decrease of current density across midnight. In detail, J_θ and J_ϕ have intensities ranging from a minimum of $-4 \cdot 10^{-8}$ A m^{-2} to a maximum of $2 \cdot 10^{-8}$ A m^{-2} and an average intensity of $1 \cdot 10^{-8}$ A m^{-2} during the 19–23 LT time interval that reduces to about half of this value during 01–05 LT with values of J_θ and J_ϕ laying within $\pm 1 \cdot 10^{-8}$ A m^{-2}. J_r varies within $-10 \div 1 \cdot 10^{-9}$ A m^{-2} before midnight and within $-0.5 \div 6 \cdot 10^{-9}$ after, its average values decreasing from around $5 \cdot 10^{-10}$ A m^{-2} to $3 \cdot 10^{-10}$A m^{-2} across midnight. These effects imply an overall decrease of total intensity of the current density after midnight in agreement with what was found previously by other authors [*Lühr et al.*, 2003a; *Ritter and Lühr*, 2006; *Shore et al.*, 2013]. The values of the horizontal components agree with *Olsen* [1997] who found intensities of $-3 \div 6 \cdot 10^{-8}$A m^{-2} at altitudes between 350 and 550 km for J_θ and *Lühr et al.* [2002] who estimated $8 \cdot 10^{-8}$A m^{-2} at an altitude of about 450 km at night. Similar to what was found by *Shore et al.* [2013] for $Dst \geq -15$ nT, our zonal component presents both eastward and westward directions after midnight, while before midnight we observe a prevalent westward direction.

Another feature emerging from Figure 2 consists of the presence, in premidnight J_r, of a pattern resembling that of the Appleton anomaly [*Lühr et al.*, 2003b]. Maxima of downward current intensity are observed at latitudes 10° ÷ 15° north and south of the dip equator as well as upward currents at the dip equator over

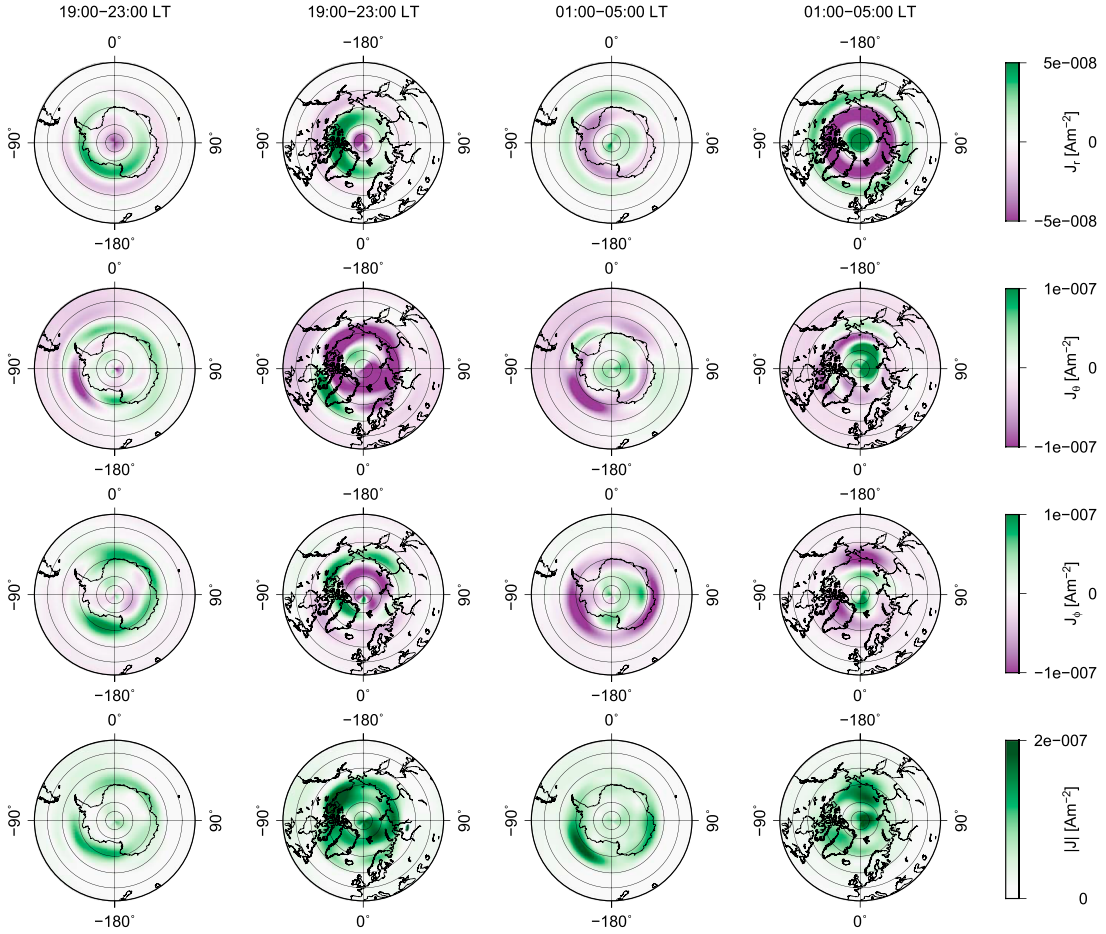

Figure 3. Same as Figure 2 but in quasi-dipole geomagnetic coordinates [*Emmert et al.*, 2010] and from a polar view. Latitudes range (first and third columns) from 40°S to 90°S for the Southern Hemisphere and (second and fourth columns) from 40°N to 90°N for the Northern Hemisphere. Circumferences are every 10°.

South America. This agrees with *Maeda et al.* [1982] who were the first to recognize in Magsat data the effects of the meridional current system associated to the equatorial electrojet.

Even if, as mentioned in section 1, data selection is based on the values of *Kp* and *Dst* indices and therefore it is optimal for low and middle latitudes, we find interesting results also for high latitudes (Figure 3). In order to obtain more representative polar latitude maps of current densities, before estimating the matrices of equations (2)–(4), we converted geographical coordinates into quasi-dipole coordinates after *Emmert et al.* [2010]. At this point we want also to call the attention of the reader to the fact that maps of Figure 3, as well as those of Figure 2, are for fixed local times (i.e., local times in the ranges 19–23 and 01–05) and should not be confused with usual polar representations, especially those of field-aligned currents, covering the entire 24 h range [*Weimer*, 2001].

From Figure 3, the structure of the field-aligned currents is clearly visible in the radial component J_r: before midnight it is outward toward the North Pole and inward toward the equator; signs reverse after midnight. At the Southern Hemisphere the structure is a mirror image. If compared to the values found by other authors, the intensity of these currents is much lower and varies in the range $\pm 2 \cdot 10^{-8}$ A m^{-2} against expected values of the order of a few μA m^{-2} [*Ohtani et al.*, 2005]. This could be ascribed both to the average (both in time and space) approach used in the analysis proposed and to the mixing of field-aligned currents activated under different conditions of interplanetary magnetic field. Another interesting feature of high-latitude current density can be observed in premidnight Northern Hemisphere J_θ and J_ϕ. Between 70°N and 80°N J_θ is characterized by a poleward current that is compatible with Pedersen currents and J_ϕ by an eastward current compatible with the equatorward portion of the Hall currents.

The currents observed at the North Pole (sunlit hemisphere) appear to be from 1.3 to 1.8 times more intense with respect to the South Pole (dark hemisphere) thus confirming the seasonal dependence of field-aligned currents found, for instance, by *Christiansen et al.* [2002].

Besides the features listed above that are found also by other authors, in Figure 2 we observe also some features more difficult to interpret. One concerns the vertical component J_r that exhibits intensities 2 orders of magnitude less than J_θ and J_ϕ, i.e., of $1 \cdot 10^{-10}$A m^{-2} and partly reverses across midnight. While the current is mostly downward during postsunset hours, it partly turns upward in the early morning. Another feature concerning J_r is the positive upward current observed over Africa during the 01–05 LT interval. This patch could relate to the high occurrence rate of spread *F* events found by *Stolle et al.* [2006] at longitudes in the band 5° ÷ 25°E and temporally well localized between mid-March and May. However, when studying the occurrence rate of spread *F* events as a function of local time, *Stolle et al.* [2006] found that local times after 01 LT are characterized by very low occurrence rates, so we can exclude ionospheric irregularities as the origin of this upward current patch. It is more likely that the structures of J_r and also that of J_θ are due to a partial representation of interhemispheric field-aligned currents. These currents are characterized by an asymmetry between winter and summer. In summer J_r is expected to flow outward in the Southern Hemisphere and inward in the Northern Hemisphere before midnight, and the opposite after midnight, while J_θ is expected to flow northward before midnight and southward after [*Yamashita and Iyemori*, 2002]. These features are clearly present before midnight in J_θ and partially in the other maps of J_θ (after midnight) and J_r (before and after midnight) shown in Figure 2. Finally, we observe that J_θ current flow mapped in Figure 2 is also consistent with that shown in *Lühr et al.* [2015, Figure 2].

4. Conclusions

The ESA Swarm mission provides a new level of observational geomagnetic data which permits to adopt a new approach in order to completely estimate the curl of the magnetic field of ionospheric origin at *F* region altitudes. This approach differs from those previously proposed [e.g., *Olsen*, 1997; *Ritter and Lühr*, 2006; *Shore et al.*, 2013] for some aspects. With respect to *Olsen* [1997] who needed to make assumptions on the variation of the horizontal components of the geomagnetic field in latitude, longitude, and height, our approach needs no assumptions. The estimation of all three components of the current density is made possible by the availability of real observations of the geomagnetic field at the different altitudes of Swarm A and B. With respect to *Ritter and Lühr* [2006] and *Shore et al.* [2013], the curl is estimated by a bin-averaged procedure rather than on orbit-by-orbit approach.

The main result of this method is the possibility to straightforwardly draw maps of density of all the components (i.e., vertical, zonal, and meridional) of the currents in the *F* region of the ionosphere during nighttime. At the light of the discussion made in section 3, the method proposed here seems promising. Results support the conclusion of *Lühr et al.* [2003a] according to which when modeling the geomagnetic field, it is not sufficient to select satellite magnetic data from dark regions to limit the effects due to currents flowing in the ionosphere. This is also shown by *Kunagu et al.* [2013] who found evidence for unmodeled signals of external origin in geomagnetic field models.

This work suggests that an optimal choice of magnetic data would require to restrict selection to postmidnight local times when *F* region electric currents, even if not absent, are weaker than before midnight. However, since such a strong decimation of data is not always affordable, maps drawn by the technique here proposed could be helpful to magnetic field modelers to select data also considering the spatial distribution of *F* region electric currents.

While some of the features of amplitudes for these large-scale (both in time and space) current intensities agree with those available in the literature, others need further investigation to understand whether they are representative of real *F* region flows or they are rather due to (a) not wholly correct removal of undesired external origin magnetic components, (b) coarse binning, and (c) average over a too wide time window. Besides looking at all local times, to shed light on the unexplained features, a natural progression of this work is the extension of the analysis with future Swarm data. With the increasing of observations it will be possible to use this technique with a smaller bin size thus being able to study smaller spatial scales and reduce the error of the averages associated to each bin. With the extension of the time window over which the analysis is performed, it will be possible to investigate current densities as a function of season. In this case it will be necessary to cope with possible effects due to spread *F* [*Stolle et al.*, 2006]. To this purpose, the use of Swarm level 2

Ionospheric Bubble Index could play a key role for selecting measurements not affected by irregularities typical of the postsunset tropical ionospheric *F* region [*Park et al.*, 2013]. Following *Green et al.* [2009], a better definition of field-aligned currents could be achieved taking into consideration different intensities of IMF and seasons, and also, this investigation will be made possible by the increase of the amount of Swarm observations. Modeling of both ionospheric currents and magnetic field as well as interpretation of magnetic measurements coming from high-resolution satellite missions would take advantage of a more accurate knowledge of the density of the radial, meridional, and zonal electric currents flowing in the ionosphere. To conclude, we want to mention that the method here proposed is suitable to estimate the curl of any kind of vector field provided that its measurements over two spherical surface are available.

Acknowledgments

We thank all members of the ESA Swarm team for their precious work, which is the basis for our investigations. Magnetic data used here are the Swarm level 1b MAGA_LR and MAGB_LR freely accessible at https://earth.esa.int/web/guest/swarm/data-access. We acknowledge the use of NASA/GSFC's Space Physics Data Facility's CDAWeb service, and OMNI data in Tsyganenko model, OMNI SW, and IMF data were obtained at http://cdaweb.gsfc.nasa.gov/. We are also grateful to the authors of CHAOS-5, MF7, and Tsyganenko models for making their models available and to two anonymous referees and to Giuseppe Consolini whose suggestions contributed to improve the manuscript. The figures were drawn with the Generic Mapping Tool [*Wessel et al.*, 2013].

The Editor thanks two anonymous reviewers for their assistance in evaluating this paper.

References

Chambodut, A., J. Schwarte, H. Lühr, and M. Mandea (2002), The selection of data in main-field modelling, paper presented at 4th OIST (Oersted International Science Team conference) Meeting, Copenhagen.

Christiansen, F., V. O. Papitashvili, and T. Neubert (2002), Seasonal variations of high-latitude field-aligned currents inferred from Ørsted and Magsat observations, *J. Geophys. Res.*, *107*(A2), 1029, doi:10.1029/2001JA900104.

Emmert, J. T., A. D. Richmond, and D. P. Drob (2010), A computationally compact representation of Magnetic-Apex and Quasi-Dipole coordinates with smooth base vectors, *J. Geophys. Res.*, *115*, A08322, doi:10.1029/2010JA015326.

Finlay, C. C., N. Olsen, and L. Tøffner-Clausen (2015), DTU candidate field models for IGRF-12 and the CHAOS-5 geomagnetic field model, *Earth Planets Space*, *67*, doi:10.1186/s40623-015-0274-3, in press.

Green, D. L., C. L. Waters, B. J. Anderson, and H. Korth (2009), Seasonal and interplanetary magnetic field dependence of the field-aligned currents for both Northern and Southern Hemispheres, *Ann. Geophys.*, *27*, 1701–1715, doi:10.5194/angeo-27-1701-2009.

Kelley, M. C. (2009), *The Earth's Ionosphere*, Academic Press, San Diego, Calif.

Kunagu, P., G. Balasis, V. Lesur, E. Chandrasekhar, and C. Papadimitriou (2013), Wavelet characterization of external magnetic sources as observed by CHAMP satellite: Evidence for unmodeled signals in geomagnetic field models, *Geophys. J. Int.*, *192*, 946–950, doi:10.1093/gji/ggs093.

Lühr, H., S. Maus, M. Rother, and D. Cooke (2002), First in-situ observation of night-time F-region currents with the CHAMP satellite, *Geophys. Res. Lett.*, *29*(10), 1489, doi:10.1029/2001GL013845.

Lühr, H., S. Maus, M. Rother, and D. Cooke (2003a), *Night-Time Ionospheric Currents*.

Lühr, H., M. Rother, S. Maus, W. Mai, and D. Cooke (2003b), The diamagnetic effect of the equatorial Appleton anomaly: Its characteristics and impact on geomagnetic field modeling, *Geophys. Res. Lett.*, *30*(17), 1906, doi:10.1029/2003GL017407.

Lühr, H., G. Kervalishvili, I. Michaelis, J. Rauberg, P. Ritter, J. Park, J. M. G. Marayo, and P. Brauer (2015), The interhemispheric and *F* region dynamo currents revisited with the Swarm constellation, *Geophys. Res. Lett.*, *42*, 3069–3075, doi:10.1002/2015GL063662.

Lui, A. T. Y. (2001), Current controversies in magnetospheric physics, *Rev. Geophys.*, *39*, 535–563, doi:10.1029/2000RG000090.

Maeda, H, T. Iyemori, T. Araki, and T. Kamei (1982), New evidence of a meridional current system in the equatorial ionosphere, *Geophys. Res. Lett.*, *9*, 337–340, doi:10.1029/GL009i004p00337.

Maus, S., F. Yin, H. Lühr, C. Manoj, M. Rother, J. Rauberg, I. Michaelis, C. Stolle, and R. D. Müller (2008), Resolution of direction of oceanic magnetic lineations by the sixth-generation lithospheric magnetic field model from CHAMP satellite magnetic measurements, *Geochem. Geophys. Geosyst.*, *9*, Q07021, doi:10.1029/2008GC001949.

Ohtani, S., G. Ueno, and T. Higuchi (2005), Comparison of large-scale field-aligned currents under sunlit and dark ionospheric conditions, *J. Geophys. Res.*, *110*, A09230, doi:10.1029/2005JA011057.

Olsen, N. (1997), Ionospheric *F* region currents at middle and low latitudes estimated from Magsat data, *J. Geophys. Res.*, *102*(A3), 4563–4576.

Olsen, N., H. Lühr, C. C. Finlay, T. J. Sabaka, I. Michaelis, J. Rauberg, and L. Tøffner-Clausen (2014), The CHAOS-4 geomagnetic field model, *Geophys. J. Int.*, *197*, 815–827, doi:10.1093/gji/ggu033.

Park, J., M. Noja, C. Stolle, and H. Lühr (2013), The Ionospheric Bubble Index deduced from magnetic field and plasma observations onboard Swarm, *Earth Planets Space*, *65*, 1333–1344, doi:10.5047/eps.2013.08.005.

Ritter, P., and H. Lühr (2006), Curl-B technique applied to Swarm constellation for determining field-aligned currents, *Earth Planets Space*, *58*, 463–476.

Shore, R. M., K. A. Whaler, S. Macmillan, C. Beggan, N. Olsen, T. Spain, and A. Aruliah (2013), Ionospheric midlatitude electric current density inferred from multiple magnetic satellites, *J. Geophys. Res.*, *118*, 5813–5829, doi:10.1002/jgra.50491.

Stolle, C., H. Lühr, M. Rother, and G. Balasis (2006), Magnetic signatures of equatorial spread *F* as observed by the CHAMP satellite, *J. Geophys. Res.*, *111*, A02304, doi:10.1029/2005JA011184.

Thomson, A. W. P., and V. Lesur (2007), An improved geomagnetic data selection algorithm for global geomagnetic field modeling, *Geophys. J. Int.*, *169*, 951–963, doi:10.1111/j.1365-246X.2007.03354.x.

Tsyganenko, N. A. (2002a), A model of the near magnetosphere with a dawn-dusk asymmetry—1. Mathematical Structure, *J. Geophys. Res.*, *107*(A7), 1179, doi:10.1029/2001JA000219.

Tsyganenko, N. A. (2002b), A model of the near magnetosphere with a dawn-dusk asymmetry—2. Parameterization and fitting to observations, *J. Geophys. Res.*, *107*(A8), 1176, doi:10.1029/2001JA000220.

Villante, U., and M. Piersanti (2008), An analysis of sudden impulses at geosynchronous orbit, *J. Geophys. Res.*, *113*, A08213, doi:10.1029/2008JA013028.

Weimer, D. R. (2001), Maps of ionospheric field-aligned currents as a function of the interplanetary magnetic field derived from Dynamics Explorer 2 data, *J. Geophys. Res.*, *106*, 12,889–12,902, doi:10.1029/2000JA000295.

Wessel, P., W. H. F. Smith, R. Scharroo, J. F. Luis, and F. Wobbe (2013), Generic Mapping Tools: Improved version released, *Eos Trans. AGU*, *94*, 409–410.

Yamashita, S., and T. Iyemori (2002), Seasonal and local time dependences of the interhemispheric field-aligned currents deduced from the Ørsted satellite and the ground geomagnetic observations, *J. Geophys. Res.*, *104*(A11), 1372, doi:10.1029/2002JA009414.